Carbon to oxygen ratios in extrasolar planetesimals

David J. Wilson[1]⋆, Boris T. Gänsicke[1], Jay Farihi[2], Detlev Koester[3]

[1] *Department of Physics, University of Warwick, Coventry CV4 7AL, UK*
[2] *University College London, Department of Physics & Astronomy, Gower Street, London WC1E 6BT, UK*
[3] *Institut für Theoretische Physik und Astrophysik, University of Kiel, 24098 Kiel, Germany*

ABSTRACT

Observations of small extrasolar planets with a wide range of densities imply a variety of planetary compositions and structures. Currently, the only technique to measure the bulk composition of extrasolar planetary systems is the analysis of planetary debris accreting onto white dwarfs, analogous to abundance studies of meteorites. We present measurements of the carbon and oxygen abundances in the debris of planetesimals at ten white dwarfs observed with the *Hubble Space Telescope*, along with C/O ratios of debris in six systems with previously reported abundances. We find no evidence for carbon-rich planetesimals, with C/O < 0.8 by number in all 16 systems. Our results place an upper limit on the occurrence of carbon-rich systems at < 17 percent with a $2\,\sigma$ confidence level. The range of C/O of the planetesimals is consistent with that found in the Solar System, and appears to follow a bimodal distribution: a group similar to the CI chondrites, with $\log(<C/O>) = -0.92$, and oxygen-rich objects with C/O less than or equal to that of the bulk Earth. The latter group may have a higher mass fraction of water than the Earth, increasing their relative oxygen abundance.

Key words: planets and satellites: composition – white dwarfs

1 INTRODUCTION

The ongoing search for extrasolar planets has been spectacularly successful, with over 1500 confirmed planets discovered to date[1], including many small objects suspected of being rocky. For a subset of these smallest detected exoplanets, both precision radial velocity measurements and transit photometry have been obtained. This provides a measurement of their masses and radii, and therefore their bulk densities. Intriguingly, these densities have a wide spread, and do not follow a simple mass-radius relationship (Weiss & Marcy 2014; Dressing et al. 2015). This may imply that some small exoplanets have compositions distinct from the rocky (and icy) planets and moons of the Solar System, which are all, to first order, a combination of H_2O, $MgSiO_3$ and Fe (Allègre et al. 2001). Modelling exoplanets with a greater variety of bulk chemistries may account for the differences in bulk densities. However, it is impossible to unambiguously infer the internal composition of a planet from its density alone. Seager et al. (2007) and Sohl et al. (2012) computed mass-radius relationships for different planetary compositions, finding a significant degeneracy between different densities, interior structures and compositions.

It has been hypothesized that enhanced C/O levels (relative to the Solar value) in a protoplanetary disc could change the condensation sequence of planetary solids, preferentially forming carbon compounds (Kuchner & Seager 2005; Moriarty et al. 2014). Under conditions where carbon is the most abundant metal, "carbon planets" may form. The alternative condensation sequence begins with the formation of CO, incorporating all of the available oxygen and restricting the formation of silicates. Excess carbon then forms SiC and graphite, for example. An Earth-sized carbon planet would likely form with an Fe-rich core, surrounded by a mantle of graphite, carbides and, at higher pressures, diamond. Bond et al. (2010) showed that this carbon-based chemistry could become important in protoplanetary discs with $C/O \gtrsim 0.8$. Carbon could contribute more than half the mass of solid exoplanets formed in such an environment, with only trace oxygen present.

Observational identification of carbon planets is hindered by the inability to measure planetary compositions in-situ, with the exception of the upper atmospheres of a few objects (Deming et al. 2013; Kreidberg et al. 2014). Given the diversity in atmospheric composition between the otherwise chemically similar terrestrial planets in the Solar System, such observations cannot be used to infer the bulk compositions of rocky exoplanets. Neither are the C/O ratios of exoplanet host stars a reliable tracer of disc composition

---

⋆ d.j.wilson.1@warwick.ac.uk
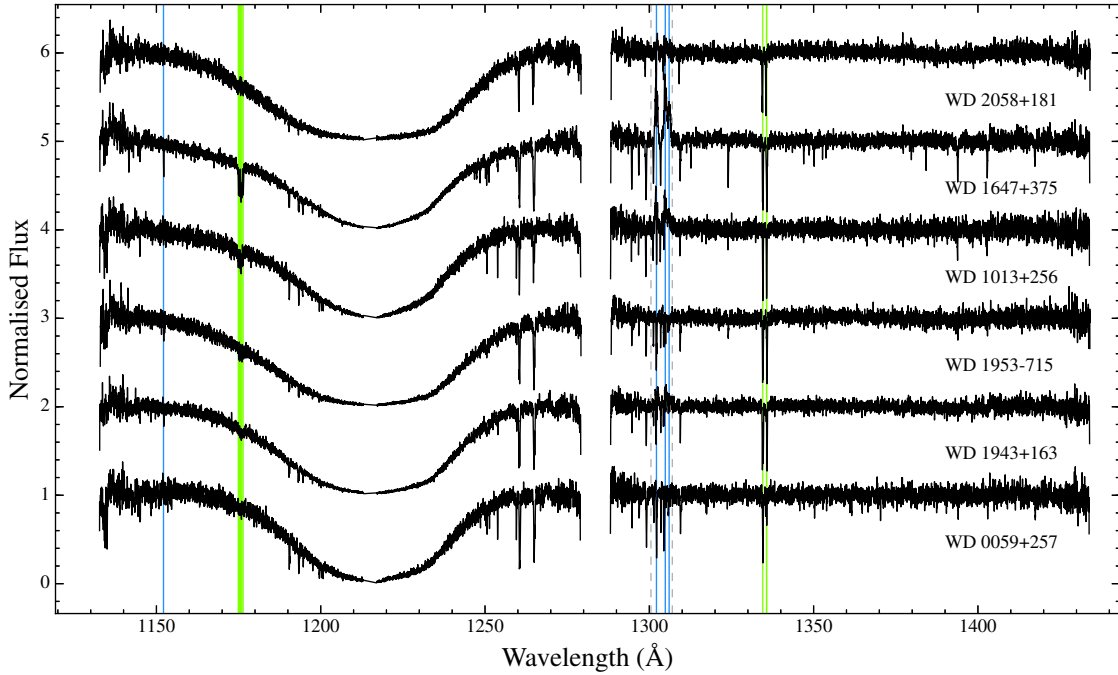[1] http://exoplanets.org/

Figure 1. *HST*/COS ultraviolet spectra of the first six white dwarfs in Table 1. Spectra are smoothed with a 5-point boxcar and normalised, then offset by multiples of 1 for clarity. The spectra are dominated by the broad Lyα line (with the central air glow emission line removed), and absorption lines of several metals are present. The wavelengths of the carbon and oxygen absorption transitions are indicated by the green and blue lines, respectively (Table 2). In some of the spectra, the area between the dashed grey lines is affected by geocoronal oxygen emission, which is not corrected for by the COS pipeline.

(Teske et al. 2013). Carbon to oxygen ratios in protoplanetary discs computed by Thiabaud et al. (2015) show only a weak dependence on the host star abundances. This ratio will also vary within a protoplanetary disc due to regional temperature variations and collisions, amongst other factors (Öberg et al. 2011; Gaidos 2015).

The only method to reliably determine compositions of exoplanetary bodies is via detection of their debris in the photospheres of white dwarfs (Zuckerman et al. 2007). Recent studies have shown that 25–50 percent of all white dwarfs are polluted by debris from planetesimals (Zuckerman et al. 2003, 2010; Koester et al. 2014a; Barstow et al. 2014), ranging in mass from small asteroids to objects as large as Pluto (Girven et al. 2012; Wyatt et al. 2014). The bulk composition of these exoplanetary bodies can be inferred from the debris detected in the white dwarf photosphere, analogous to how the compositions of Solar System bodies are inferred from meteorites (Lodders & Fegley 2011). High-resolution spectroscopy of over a dozen metal-polluted white dwarfs has revealed accretion of numerous atomic species, allowing detailed studies of the chemical composition of extrasolar planetesimals (Klein et al. 2011; Gänsicke et al. 2012; Dufour et al. 2012; Jura et al. 2012; Farihi et al. 2013; Xu et al. 2014; Raddi et al. 2015; Wilson et al. 2015). Overall, these objects have chemical compositions similar to inner Solar System bodies, dominated by O, Si, Mg and Fe, and volatile depleted (Jura & Young 2014). However, the detailed compositions can be very diverse, with objects having enhanced levels of core material (Melis et al. 2011; Gänsicke et al. 2012; Wilson et al. 2015), evidence of post-nebula pro-

cessing (Xu et al. 2013), and significant mass fractions of water (Farihi et al. 2013; Raddi et al. 2015).

Thus far, studies of planetesimal compositions at white dwarfs have predominately focused on individual objects. However, the growing sample of abundance studies now allows conclusions to be derived regarding the overall chemical abundances of (solid) exoplanet precursors in a statistically significant sample of systems. Here, we use these data to constrain the occurrence frequency of carbon planets.

2 CARBON AND OXYGEN DEBRIS ABUNDANCES AT WHITE DWARFS

We present debris abundance measurements for ten white dwarfs observed with the Cosmic Origins Spectrograph on board the *Hubble Space Telescope* (*HST*/COS) as part of Program IDs 12169, 12869, and 12474 (Gänsicke et al. 2012; Koester et al. 2014a). Table 1 presents their effective temperatures ($T_{\rm eff}$) and surface gravities ($\log g$), as well as elemental accretion rates. The techniques used to determine these results are described in detail in Koester et al. (2014a), so we only briefly summarise here. Firstly, optical spectra from the SPY survey were refitted with the latest model grid to determine temperatures and surface gravities. If no SPY spectra were available, we used parameters from Gianninas et al. (2011). After correcting for a small systematic difference between the two determinations, we fixed the surface gravity to the value obtained from the optical data, and then determined the temperature from a fit to the ultraviolet COS spectra. For this we used the slope between

Table 1. New atmospheric parameters and debris accretion rate measurements for ten white dwarfs identified by Koester et al. (2014a). Spectra of the first six are shown in Fig. 1. [1]Updated from Gänsicke et al. (2012)

| Name	T_{eff} (K)	$\log g$ (cm s^{-2})	$\dot{M}$(C) (g s^{-1})	$\dot{M}$(O) (g s^{-1})
WD 2058+181	17308 ± 235	7.920 ± 0.089	$(2.06 \pm 0.95) \times 10^6$	$(1.03 \pm 0.47) \times 10^7$
WD 1647+375	22803 ± 310	7.902 ± 0.089	$(1.14 \pm 0.52) \times 10^7$	$(2.16 \pm 0.75) \times 10^8$
WD 1013+256	22133 ± 301	8.022 ± 0.089	$(1.92 \pm 0.66) \times 10^6$	$(3.2 \pm 1.6) \times 10^7$
WD 1953–715	18975 ± 258	7.957 ± 0.089	$(1.56 \pm 0.72) \times 10^6$	$(2.8 \pm 1.3) \times 10^7$
WD 1943+163	19451 ± 264	7.896 ± 0.089	$(1.40 \pm 0.64) \times 10^6$	$(1.97 \pm 0.91) \times 10^7$
WD 0059+257	20491 ± 278	8.002 ± 0.089	$\leq 2.9 \times 10^4$	$(3.4 \pm 1.6) \times 10^7$
PG 0843+516[1]	22412 ± 304	7.902 ± 0.089	$(2.42 \pm 1.11) \times 10^5$	$(1.09 \pm 0.50) \times 10^8$
PG 1015+161[1]	18911 ± 257	8.042 ± 0.089	$\leq 6.9 \times 10^4$	$(4.9 \pm 2.3) \times 10^7$
SDSS J1228+1040[1]	20713 ± 281	8.150 ± 0.089	$(1.70 \pm 0.78) \times 10^5$	$(4.4 \pm 2.0) \times 10^8$
GALEX J1931+0117[1]	21457 ± 291	7.900 ± 0.089	$(7.1 \pm 4.9) \times 10^5$	$(9.0 \pm 6.2) \times 10^8$
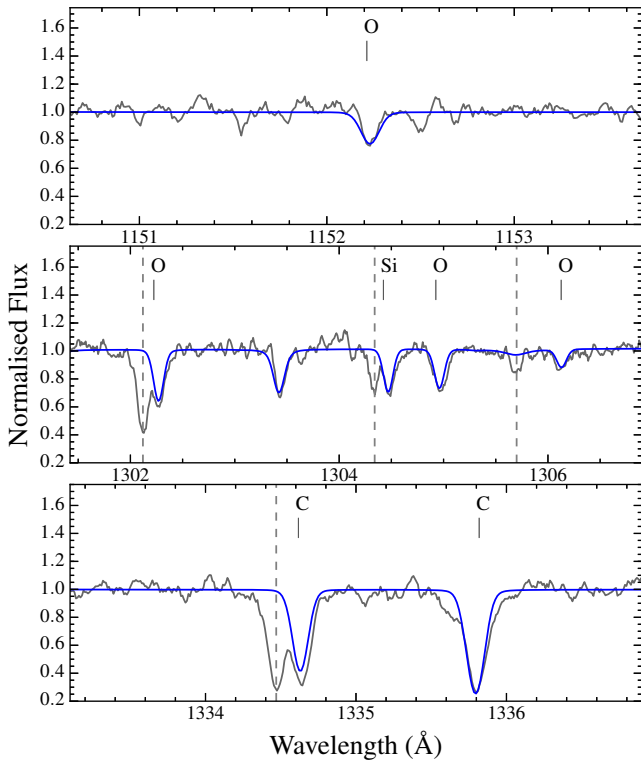
Figure 2. Enlarged sections of the spectrum of WD 1953–715 showing photospheric O I 1152.2, 1302.2, 1304.9, 1306.0 Å, Si II 1304.4 Å and C II 1334.5, 1335.6 Å absorption lines. The model atmosphere fit used to calculate the abundances is overlaid in blue. Interstellar components of the O I 1302.2 Å, Si II 1304.4, 1305.6 Å and C II 1334.5 Å absorption lines are marked with dashed grey lines.

Table 2. List of the absorption lines used for the debris abundance measurements.

Ion	Vacuum rest wavelength (Å)
C II	1334.530, 1335.660, 1335.708
C III	1174.930, 1175.260, 1175.590, 1175.710, 1175.987, 1176.370
O I	1152.150, 1302.170, 1304.860, 1306.030

the optical photometry and the absolutely calibrated COS spectra as additional constraint.

The best fit atmospheric parameters were then used to create synthetic spectra containing approximately 14 000 spectral lines from 14 elements. The atmospheric metal abundances were varied until a good fit was obtained between the synthetic spectra and the observed absorption lines. Adjusting the abundances by ± 0.2 dex around the best fit values allowed an estimate of the abundance uncertainties. The uncertainty in the atmospheric parameters has only a small effect on the element abundances (<0.04 dex). Table 2 lists the absorption lines used to determine the carbon and oxygen abundances. The oxygen abundances are primarily measured from the O I 1152.15 Å line. The O I lines around 1300 Å are affected by geocoronal emission in several of the spectra, which is not corrected for by the COS pipeline. Where no geocoronal emission is present, these lines are still affected by blending with Si II and interstellar O I lines, but still provide (less accurate) abundance determinations which agree with measurements from the O I 1152.15 Å line.

As the metals diffuse out of the white dwarf atmosphere on different time scales, the element abundances in the white dwarf photosphere do not necessarily match those of the debris material. The diffusion time scales were calculated using the same atmospheric models as for the spectral fitting (Koester 2009). As the diffusion time scales for these hydrogen atmosphere white dwarfs are of order days to, at most, months, it is reasonable to assume that the white dwarfs are currently accreting, and accretion and diffusion are in equilibrium. The accretion rate is therefore the ratio of the atmospheric abundance to the diffusion time scale. Radiative levitation, which can change the diffusion time scales or even keep an element in the atmosphere without ongoing accretion (Chayer & Dupuis 2010), is taken into account when calculating the diffusion time scales, but has a negligible effect on carbon and no effect on oxygen over the temperature range of our sample. Finally, the C/O ratio by number is calculated as the ratio of the accretion rates, weighted by the relative atomic masses.

Analysis of the debris in four of these white dwarfs were presented in Gänsicke et al. (2012), but the abundances used here have been updated with new calculations. Ultraviolet spectra of the remaining six white dwarfs are shown in Fig. 1, featuring photospheric absorption lines from a variety of metals, including both carbon and oxygen (Fig. 2).

In addition to these new measurements, we have assembled all published abundances for carbon and oxygen at white dwarfs both observed with COS and analysed with the same model described above (Wilson et al. 2015; Xu et al. 2014; Farihi et al. 2013; Xu et al. 2013). These criteria create a homogeneous sample, which avoids systematic uncertainties that may result from comparing different data sources and models. Where more than one measurement is available we use the most recent result, and we adopt the most commonly used white dwarf designations. In total, we discuss C/O measurements for debris in eleven systems and firm upper limits for another five.

Four of the white dwarfs in our sample have helium dominated atmospheres, labelled in Fig 3 and Table 3. These stars develop deep convective envelopes, which may lead to dredge-up of core-carbon into the atmosphere. Dredge-up typically occurs in cool ($T_{\rm eff} \lesssim 12\,000\,{\rm K}$) white dwarfs, but it has been suggested that a small number of white dwarfs may have helium envelopes thin enough to pollute the atmosphere with core-carbon even at higher temperatures (Koester et al. 2014b; Wilson et al. 2015). Thus, although we treat the C/O ratios in helium atmosphere white dwarfs as firm detections, this caveat should be kept in mind when discussing the planetary abundances at individual white dwarfs. The majority of our sample (12 out of 16) have hydrogen atmospheres, which are unaffected by dredge up.

3 DISCUSSION

Figure 3 and Table 3 show the C/O ratios of the planetesimal debris at the 16 systems in our sample as a function of effective temperature (and therefore the age since white dwarf formation). We compare these ratios with those for the CI chondritic meteorites (Lodders & Fegley 2011), bulk Earth (Allègre et al. 2001), Comet Halley (Jessberger et al. 1988), and the Solar photosphere (Asplund et al. 2009). As carbon chemistry is thought to become an important factor in protoplanetary discs with C/O > 0.8 ($\log{\rm (C/O)} > -0.097$), we take this as a lower limit for a planetesimal formed in a carbon-rich environment. We note, however, that planets formed in such discs are predicted to potentially have C/O ≫ 1.0 (Bond et al. 2010).

We find no planetary debris with C/O > 0.8. The debris at WD 2058+181 has the highest ratio, with $\log{\rm (C/O)} = -0.57 \pm 0.28$, still below the Solar value. Applying binomial statistics, we find that planetesimals with C/O > 0.8 occur in < 17 percent of systems at a $2\,\sigma$ confidence level, falling to < 6.5 percent with $1\,\sigma$ confidence. Our upper limit on high planetary C/O is consistent with that found in stellar abundances by Fortney (2012), who showed that the fraction of stars with C/O > 0.8 is no more than 10–15 percent. None of the planetesimal debris in the 16 systems has C/O similar to that of Comet Halley ($\log{\rm (C/O)} = -0.04$), supporting the conclusions of Veras et al. (2014) that comets are not a significant population of parent bodies for the debris detected at many white dwarfs. There are no observed trends in C/O with the post-main sequence (cooling) age.

Although none of the systems are carbon-rich, the material does appear to fall into two distinct populations, with an apparent gap between $\log{\rm (C/O)} \approx -1$ and $\log{\rm (C/O)} \lesssim$

−2. Six systems have relatively high C/O ratios, with $\log({\rm <C/O>}) = 0.12 \pm 0.07$ (where the error is the 1σ spread). This is consistent with the CI chondrite meteorites (Lodders & Fegley 2011), which are thought to be representative of the primordial composition of the rocky Solar System. It is likely that the debris in these systems originated as small asteroids, which had not undergone significant post-nebula differentiation .

The remaining ten systems all have C/O less than or equal to that of the bulk Earth. Comparing the relative abundances of carbon and oxygen in this group with the other elements detected in their debris shows that they have a high oxygen abundance (relative to, for example, Si), rather than being relatively poor in carbon. A speculative explanation for this is that the parent bodies of the debris contained a significant amount of water, similar to Ceres or the large moons of the gas giants. High mass fractions of water have already been detected in debris at GD 61 (Farihi et al. 2013), which has an upper limit on its C/O ratio placing it in the low C/O group. Addition of water to a planetesimal with an otherwise Earth-like composition would increase the abundance of oxygen, but leave the carbon abundance unchanged, decreasing the C/O ratio. A potential caveat to this argument is the study by Jura & Xu (2012) of hydrogen in helium atmosphere white dwarfs in the 80 pc sample. Their results suggested that water makes up less that one percent of the mass accreting onto the white dwarfs in their sample. However, both the amount and origin of hydrogen in helium atmosphere white dwarfs, and its relevance to debris accretion, are subject to ongoing discussion (Koester & Kepler 2015; Bergeron et al. 2011).

Additionally, the carbon content of the Earth, and in particular the core, is still subject to discussion. Allègre et al. (2001) find a mass fraction of 0.17–0.36 percent, the lower bound of which we use to calculate a C/O ratio in Fig. 3. In contrast, Marty (2012) instead calculate a carbon mass fraction of only 0.053 percent. Using the oxygen fraction from Allègre et al. (2001), this lowers the $\log({\rm <C/O>}$ to -2.7, consistent with the average of the low C/O systems ($\log({\rm <C/O>}) = -2.5 \pm 0.36$).

By providing a strong lower limit of the occurrence of carbon-rich planetesimals, we show that debris-polluted white dwarfs are likely the most powerful diagnostics of carbon chemistry in extrasolar planetesimals, and increasing the sample size will provide stronger constraints on the existence, or lack thereof, of carbon planets. More generally, abundance studies of the debris at white dwarfs are sensitive to a wide variety of elements, making them the ideal tool to systematically investigate the full range of non-gaseous planetary chemistry.
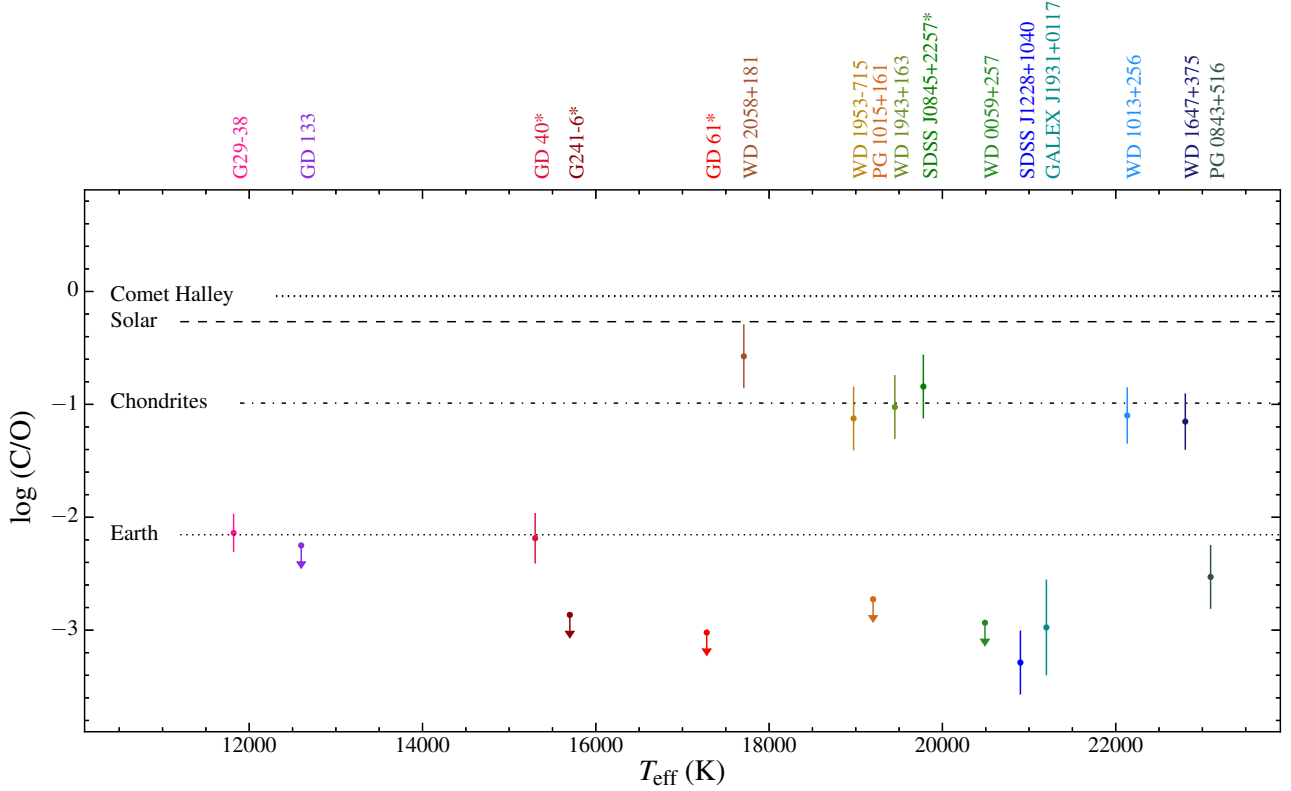
Figure 3. C/O number ratios of the planetesimal debris in our sample, plotted against the effective temperature ($T_{\rm eff}$) of the host white dwarfs and compared with various Solar System bodies. The colour scheme is intended to aid identification and has no physical significance. White dwarfs with helium atmospheres, which may be affected by convective carbon dredge-up that could enhance their carbon abundances (Sect. 2), are marked with *. Objects with similar temperatures have been offset slightly for clarity. Whilst we plot the value for Earth's C/O from Allègre et al. (2001), we note that Marty (2012) suggests a value ≈ 0.5 dex lower (Sect. 3).

.

Table 3. C/O ratios by number shown in Fig. 3, in order of increasing C/O. White dwarfs with helium atmospheres are marked with *. References: 1. This work; 2. Xu et al. (2013); 3. Farihi et al. (2013); 4. Xu et al. (2014); 5. Wilson et al. (2015).

Name	$\log{\rm (C/O)}$	Ref.
SDSS J1228+1040	-3.3 ± 0.28	1
GD 61*	≤ -3.0	3
GALEX J1931+0117	-3.0 ± 0.42	1
WD 0059+257	≤ -2.9	1
G241-6*	≤ -2.9	2
PG 1015+161	≤ -2.7	1
PG 0843+516	-2.5 ± 0.28	1
GD 13	≤ -2.2	4
GD 40*	-2.2 ± 0.22	2
G29-38	-2.1 ± 0.17	4
WD 1647+375	-1.2 ± 0.25	1
WD 1013+256	-1.1 ± 0.25	1
WD 1953-715	-1.1 ± 0.28	1
WD 1943+163	-1.0 ± 0.28	1
SDSS J0845+2257*	-0.84 ± 0.28	5
WD 2058+181	-0.57 ± 0.28	1

REFERENCES

Allègre C., Manhès G., Lewin E., 2001, Earth and Planetary Science Letters, 185, 49

Asplund M., Grevesse N., Sauval A. J., Scott P., 2009, ARA&A, 47, 481

Barstow M. A., Barstow J. K., Casewell S. L., Holberg J. B., Hubeny I., 2014, MNRAS, 440, 1607

Bergeron P., et al., 2011, ApJ, 737, 28

Bond J. C., O'Brien D. P., Lauretta D. S., 2010, ApJ, 715, 1050

Chayer P., Dupuis J., 2010, in Werner K., Rauch T., eds, American Institute of Physics Conference Series Vol. 1273, American Institute of Physics Conference Series. pp 394–399 (arXiv:1010.2518), doi:10.1063/1.3527849

Deming D., et al., 2013, ApJ, 774, 95

Dressing C. D., et al., 2015, ApJ, 800, 135

Dufour P., Kilic M., Fontaine G., Bergeron P., Melis C., Bochanski J., 2012, ApJ, 749, 6

Farihi J., Gänsicke B. T., Koester D., 2013, Science, 342, 218

Fortney J. J., 2012, ApJ Lett., 747, L27

Gaidos E., 2015, ApJ, 804, 40

Gänsicke B. T., Koester D., Farihi J., Girven J., Parsons S. G., Breedt E., 2012, MNRAS, 424, 333

Gianninas A., Bergeron P., Ruiz M. T., 2011, ApJ, 743, 138

Girven J., Brinkworth C. S., Farihi J., Gänsicke B. T., Hoard D. W., Marsh T. R., Koester D., 2012, ApJ, 749, 154

Jessberger E. K., Christoforidis A., Kissel J., 1988, Nat, 332, 691

Jura M., Xu S., 2012, AJ, 143, 6

Jura M., Young E. D., 2014, Annual Review of Earth and Planetary Sciences, 42, 45

Jura M., Xu S., Klein B., Koester D., Zuckerman B., 2012, ApJ, 750, 69

Klein B., Jura M., Koester D., Zuckerman B., 2011, ApJ, 741, 64

Koester D., 2009, A&A, 498, 517

Koester D., Kepler S. O., 2015, A&A, 583, A86

Koester D., Gänsicke B. T., Farihi J., 2014a, A&A, 566, A34

Koester D., Provencal J., Gänsicke B. T., 2014b, A&A, 568, A118

Kreidberg L., et al., 2014, Nat, 505, 69

Kuchner M. J., Seager S., 2005, preprint, (arXiv:0504214)

Lodders K., Fegley B., 2011, Chemistry of the Solar System. RSC Publishing, Cambrige

Marty B., 2012, Earth and Planetary Science Letters, 313, 56

Melis C., Farihi J., Dufour P., Zuckerman B., Burgasser A. J., Bergeron P., Bochanski J., Simcoe R., 2011, ApJ, 732, 90

Moriarty J., Madhusudhan N., Fischer D., 2014, ApJ, 787, 81

Öberg K. I., Murray-Clay R., Bergin E. A., 2011, ApJ Lett., 743, L16

Raddi R., Gänsicke B. T., Koester D., Farihi J., Hermes J. J., Scaringi S., Breedt E., Girven J., 2015, MNRAS, 450, 2083

Seager S., Kuchner M., Hier-Majumder C. A., Militzer B., 2007, ApJ, 669, 1279

Sohl F., Wagner F. W., Rauer H., 2012, preprint, (arXiv:1211.3331)

Teske J. K., Cunha K., Schuler S. C., Griffith C. A., Smith V. V., 2013, ApJ, 778, 132

Thiabaud A., Marboeuf U., Alibert Y., Leya I., Mezger K., 2015, A&A, 580, A30

Veras D., Shannon A., Gänsicke B. T., 2014, MNRAS, 445, 4175

Weiss L. M., Marcy G. W., 2014, ApJ Lett., 783, L6

Wilson D. J., Gänsicke B. T., Koester D., Toloza O., Pala A. F., Breedt E., Parsons S. G., 2015, MNRAS, 451, 3237

Wyatt M. C., Farihi J., Pringle J. E., Bonsor A., 2014, MNRAS, 439, 3371

Xu S., Jura M., Klein B., Koester D., Zuckerman B., 2013, ApJ, 766, 132

Xu S., Jura M., Koester D., Klein B., Zuckerman B., 2014, ApJ, 783, 79

Zuckerman B., Koester D., Reid I. N., Hünsch M., 2003, ApJ, 596, 477

Zuckerman B., Koester D., Melis C., Hansen B. M., Jura M., 2007, ApJ, 671, 872

Zuckerman B., Melis C., Klein B., Koester D., Jura M., 2010, ApJ, 722, 725

This paper has been typeset from a TEX/LATEX file prepared by the author.